AIP | Applied Physics Letters

Ferroelectric domains and piezoelectricity in monocrystalline Pb(Zr,Ti)O3 nanowires

J. Wang, C. S. Sandu, E. Colla, Y. Wang, W. Ma et al.

Citation: Appl. Phys. Lett. **90**, 133107 (2007); doi: 10.1063/1.2716842
View online: http://dx.doi.org/10.1063/1.2716842
View Table of Contents: http://apl.aip.org/resource/1/APPLAB/v90/i13
Published by the AIP Publishing LLC.

Ferroelectric domains and piezoelectricity in monocrystalline $Pb(Zr,Ti)O_3$ nanowires

J. Wang, C. S. Sandu, E. Colla, Y. Wang, W. Ma, R. Gysel, H. J. Trodahl,[a] and N. Setter[b]
Ceramics Laboratory, Swiss Federal Institute of Technology (EPFL), 1015 Lausanne, Switzerland

M. Kuball
H. H. Wills Physics Laboratory, University of Bristol, Bristol BS8 1TL, United Kingdom

(Received 18 November 2006; accepted 21 February 2007; published online 27 March 2007)

Monocrystalline lead zirconate titanate nanowires were grown by a polymer assisted solvothermal technique. X-ray and electron diffractions confirmed tetragonal perovskite structure and a [001] orientation along the wire axis, respectively. Raman scattering was used to analyze the structure and composition of single wires. Ferroelectric/ferroelastic domain walls were imaged by transmission electron microscopy, showing some domains with polarization directions along the wire axis and some perpendicular to it. The domain walls disappeared upon heating above the ferroelectric phase transition at 460 °C. Ferroelectric switching, as well as piezoelectric activity and hysteresis, were shown locally using piezoelectric force microscopy. © *2007 American Institute of Physics*.
[DOI: 10.1063/1.2716842]

Piezoelectric materials are being used and further investigated for a wide range of applications, from medical, environmental, and industrial process monitoring to robotics, energy harvesting, and high frequency communication systems.[1] Due to their important sensing and actuating capabilities, they are of interest also for eventual nanoelectromechanical systems.[2] Ferroelectric perovskites constitute the most useful group of piezoelectric ceramics due to their large piezoelectric coefficients and electromechanical coupling coefficients.[3] The synthesis of ferroelectric nanowires and nanotubes has been reported for some 6 years. Those included several perovskites such as $BaTiO_3$,[4,5] $SrTiO_3$,[4,5] $KNbO_3$,[6] $PbTiO_3$,[7] and $Pb(Zr,Ti)O_3$ (PZT).[8,9] Synthesis methods include infiltration,[10–14] molten salt technique,[15] electrophoresis,[16] solvothermal,[6] and others.

While synthesis routes are understood to a certain extent, piezoelectric properties of monocrystalline ferroelectric nanowires have hardly been reported. Urban *et al.* reported ferroelectric switching in $BaTiO_3$ (Ref. 5) and recently observed the ferroelectric phase transition in a single wire of $BaTiO_3$.[17] Suyal *et al.* reported piezoelectric hysteresis and domain structure in $KNbO_3$ wires.[18] Very recently, Wang *et al.* reported piezoelectric properties of monocrystalline nanowires of $BaTiO_3$.[19] Those are the only reports on piezoelectric properties of single crystal nanowires. A few more reports exist on piezoelectricity in polycrystalline submicrometer wires and tubes prepared by the infiltration techniques (e.g., Ref. 20). While PZT is the most important piezoelectric ceramic with extensive and wide applications, functional properties of PZT single crystal nanowires have not been reported so far. The properties are of interest for fundamental understanding, since first principle calculations show a promise of interesting size effects,[21] and for evaluating the potential use of the material. Moreover, the domain structure of nanowires is hardly known, and this is especially missing in PZT where, in the bulk form, domain wall movements contribute substantially to the piezoelectric activity of the material.[1] The work reported here fills some of the missing knowledge.

The one-dimensional PZT particles were produced by a hydrothermal method.[9] 0.08 mol l^{-1} $(C_4H_9O)_4Ti$ ethanol solution was introduced into 0.10 mol l^{-1} $ZrOCl_2$ water solution under stirring to form a transparent mixed solution, from which zirconium and titanium hydroxide (ZTOH) was subsequently coprecipitated by 0.15 mol l^{-1} ammonia solution. The ZTOH precipitate was filtered and washed with de-ionized water six times and then redispersed in de-ionized water under strong stirring, followed by the addition of $Pb(NO_3)_2$, KOH, and the poly(vinyl alcohol) (PVA) solution. The concentrations in the final feedstock are 0.10 mol l^{-1} for ZTOH, 0.11 mol l^{-1} for $Pb(NO_3)_2$, 1.5 mol l^{-1} for KOH, and 0.4 g l^{-1} for PVA. The sufficiently stirred feedstock was charged into a 50 ml stainless-steel Teflon-lined autoclave with a fill factor of 80 vol % and then underwent a hydrothermal treatment at 200 °C for 24 h. The products were filtered and washed by de-ionized water and absolute ethanol, and dried at 45 °C in air for 12 h. The x-ray diffraction pattern, obtained with a Siemens Kristalloflex diffractometer, indicated a pure tetragonal perovskite phase of the products.

Raman spectra were measured with a Renishaw InVia Raman microscope using 488 nm excitation. The focus was about 0.5 μm; spectra from nanowires with substantially smaller diameters required correction for the Raman signal from the sapphire substrate. The power level was varied to establish that there was minimal heating of the nanowires and for the data presented here was held below 1 mW. The spectra were all collected at ambient temperature with a resolution of about 1 cm^{-1}.

Raman spectra from opposite ends of a typical wire are shown in Fig. 1. In common with all of the spectra, including for wires with diameters well below the diffraction limit, the pattern is clearly that of tetragonal PZT.[1] It is notable that the features near 350 and 630 cm^{-1} differ in the two spectra, indicating that the composition varies along the wire.[22] The zirconium composition index x can be determined from these

[a]Permanent address: Victoria University, Wellington, New Zealand.
[b]Electronic mail: nava.setter@epfl.ch

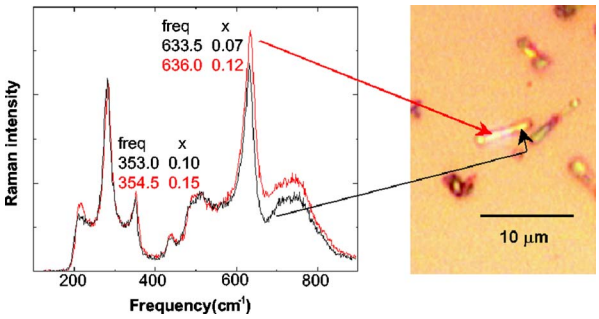

FIG. 1. (Color online) Raman spectra from opposite ends of a typical wire. The zirconium content (x) is determined according to frequency of the two composition-sensitive peaks (Ref. 22) and shows a composition gradient along the wire.

measurements to an accuracy of about 0.03, with the best accuracy from the 630 cm^{-1} line, and can be seen to vary from 0.08 to 0.13 along this particular wire. Across the entire ensemble of wires we found x varying from 0.05 to 0.3.

The microstructure of the particles was examined by scanning electron microscopy (SEM) on a Philips XL 30, and by transmission electron microscopy (TEM) on a Philips CM 300 equipped with a field emission gun at an accelerating voltage of 300 kV and on a Hitachi HF-2000 equipped with heating holder. The base pressure during the heating was 2×10^{-6} Pa.

The one-dimensional structures show diameters varying between 80 nm and 2 μm and lengths of several microns, as determined from SEM images. The monocrystallinity was confirmed for all the nanowires checked by the TEM and the directions of the crystal plane have been established from the high resolution TEM images (not shown here). In all the studied nanowires, [001] was parallel to the growth direction, along the axis of the wire. The ratio c/a of the lattice constants has been found to be $\sim1.03\pm0.01$. The TEM images of a typical nanowire are shown in Fig. 2. In the as-grown nanowire [Fig. 2(a)] a dark line could be observed along the nanowire axis. This contrast line disappeared when the nanowire was heated above 460 °C and reappeared upon cooling back to room temperature. Ferroelectric domain walls (at 45° to the nanowire axis) appeared after the first thermal cycling, when the temperature decreased below 400 °C [Fig. 2(b)]. These domains disappeared when the sample was reheated above 460 °C.

Differential scanning calorimetry measurements were done using a Setaram apparatus with a heating rate of

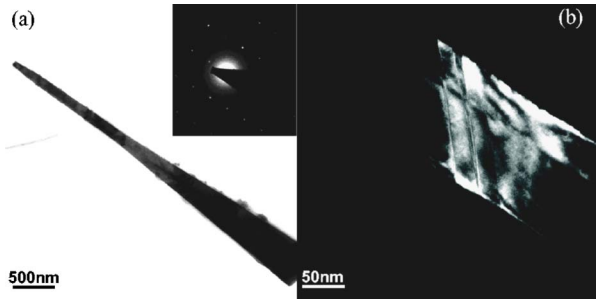

FIG. 2. (Color online) TEM images of the PZT nanowires showing (a) bright field image of a pristine nanowire and (b) dark field image of a wire cooled to RT after heating to 480 °C. Domain walls are seen at 45° to the wire axis which lies along [001].

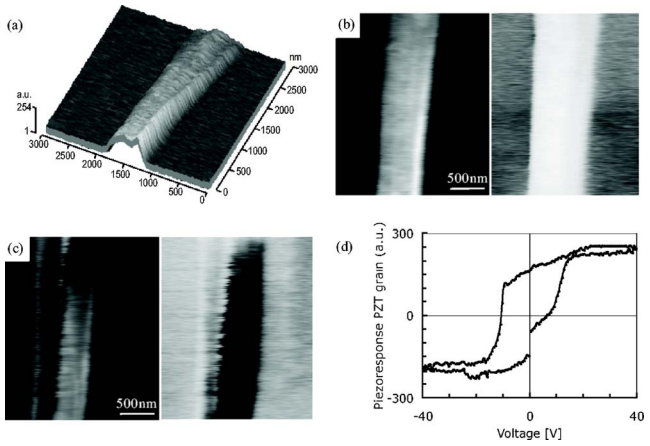

FIG. 3. (a) 3D plot of the amplitude of the piezoelectric response of a pristine PZT nanowire. Amplitude (left) and phase (right) of the piezoelectric response of the nanowire poled with voltages of (b) −40 V and (c) +55 V applied to the bottom electrode. (d) Local positive hysteresis loop of the piezoelectric response in the stably active part of the nanowire. (The AFM tip scanned one line under a certain dc bias with a frequency of 0.4 Hz. The piezoelectric response of the "poled" line was measured consecutively under zero bias. The "poling" and measuring steps were repeated to collect a complete piezoelectric loop.)

10 K/min. An exothermal peak was observed between 450 and 500 °C, upon heating, in heat flow curve. The thermal energy change was of about 0.56 J/g. This could correspond to the tetragonal-cubic phase transformation, which was observed by *in situ* TEM investigation at about 460 °C in the nanowires. However, this fact did not repeat itself upon recycling of samples and will need additional investigation prior to further interpretation.

Piezoelectric force microscopy (PFM) was employed to study the local piezoelectric response of the PZT nanowires. Contact mode PFM must be used in order to apply the electric field onto the piezoelectric nanowires. The small particles must therefore be fixed to the conductive substrate to avoid uncontrolled displacement of the particle during the scanning movement of the tip (push effects). The nanowires were therefore attached to a conductive substrate as described in Ref. 18.

The converse piezoelectric effect is excited by applying an ac electric field between the substrate electrode and the conductive atomic force microscope (AFM) tip, which scans the bare upper surface of the ferroelectric object. The amplitude of the detected piezoelectric vibration is related to the piezoelectric coefficient of the material whereas the phase of the signal can reflect the polarization direction. Manipulations of the polarization state are generally achieved by imposing a stronger dc field. The field, as a consequence of the particular geometry of the tip as an electrode, is not uniform and quantitative results are therefore difficult. Figure 3(a) shows the amplitude of the piezoelectric vibration in a three-dimensional (3D) plot, measured on a pristine nanowire by collecting the piezoelectric response component in the out of plane direction. The bright area represents the piezoelectrically active region and delimits the nanowire shape on the piezoelectrically inactive substrate (dark color). The actual diameter of that nanowire as checked with SEM is about 200 nm, which has been enlarged due to the geometry of the AFM tip. Polarization switching experiments were performed. Figures 3(b) and 3(c) show the maps of amplitude and phase of piezoelectric response taken immediately after

applying −40 and +55 V dc biases on the scanned region by the AFM tip along the out of plane direction, respectively. The piezoelectric activity is seemingly perpendicular to the polarization direction, but it should be noted that due to the geometry of the measured nanowires, there is a tilt angle between the nanowire axis (polarization direction) and the horizontal substrate plane which leads to the manifestation of the out of plane piezoelectric activity.

By comparing the amplitude maps in Figs. 3(b) and 3(c), it can be noted that only the right half of the nanowire shows sufficient activity and complete switching; therefore, the switching behavior study was limited to this part of the wire. The piezoelectric response loop shown in Fig. 3(d) was obtained with a positive voltage cycle on a negatively prepoled area of this active part. It shows a typical piezoelectric hysteresis. In our measurement, the contact between the particle and the bottom electrode could be unstable due to the variations of the electrostatic force between the tip and the surface charges of the particle under different dc voltages. In addition, the mechanical force between the tip and the particle could degrade the contact. Therefore, it will be uncautious to say that the left side of the nanowire [Fig. 3(c)] is not ferroelectric. Of importance is that at least part of the nanowire (its right side) shows a significant piezoelectric activity and can be switched.

The observed [001] orientation, namely, polarization direction along the axis of the nanowire, agrees with the expectations, as it minimizes the depolarization field. 180° domains, all with polarization vectors along the wire axis, are then expected. Compositional gradient along the axis may induce self-polarization along the wire.[23] In addition, the gradual change of the lattice constant due to compositional gradient can cause self-polarization due to the flexoelectric effect.[24] Self-polarization may be advantageous for potential future piezoelectric applications.

Moreover, taking into account the [001] orientation of the axis of the wires, the orientation of the domain walls [Fig. 2(b)] after annealing clearly indicates flipping of the polar axis by 90°. Combining this with the manifestation of 180° switching during the piezoelectric force microscopy study, it is reasonable to conclude that the domain walls are active and likely to contribute to the piezoelectric response, as is the case in bulk ceramics. This may be of a practical importance for possible future applications.

In conclusion, hydrothermally synthesized tetragonal monocrystalline PZT nanowires having a [001] orientation along the wire axis manifested ferroelectric phase transition and formation of polydomains with 90° domain walls, which disappear upon heating above the ferroelectric phase transition temperature. The wires are piezoelectrically active and manifest piezoelectric hysteresis and polarization switching.

MIND (EU-FP6), COST-539 (Swiss Federal Office of Education and Science), and NCCR "Nanoscience" (Swiss National Science Foundation) are acknowledged for financial support. The authors thank J. W. Pomeroy (Bristol) for contributions to the Raman measurements. CIME (electron microscopy center of EPFL) is acknowledged for generously allowing the authors to use their facilities.

[1] *Piezoelectric Materials in Devices*, edited by N. Setter (Ceramics Laboratory, Lausanne, 2002).
[2] Z. L. Wang and J. H. Song, Science **312**, 242 (2006).
[3] *Piezoelectric Materials in Devices*, edited by N. Setter (Ceramics Laboratory, Lausanne, 2002), Chap. 1, pp. 1–28.
[4] Y. B. Mao, S. Banerjee, and S. S. Wong, Chem. Commun. (Cambridge) 408 (2003).
[5] J. J. Urban, W. S. Yun, Q. Gu, and H. Park, J. Am. Chem. Soc. **124**, 1186 (2002).
[6] J. F. Liu, X. L. Li, and Y. D. Li, J. Nanosci. Nanotechnol. **2**, 617 (2002).
[7] Y. M. Hu, H. S. Gu, X. C. Sun, J. You, and J. Wang, Appl. Phys. Lett. **88**, 193120 (2006).
[8] S.-B. Cho, M. Oledzka, and R. E. Riman, J. Cryst. Growth **226**, 313 (2001).
[9] G. Xu, Z. H. Ren, P. Y. Du, W. J. Weng, G. Shen, and G. R. Han, Adv. Mater. (Weinheim, Ger.) **17**, 907 (2005).
[10] Y. Luo, I. Szafraniak, N. D. Zakharov, V. Nagarajan, M. Steinhart, R. B. Wehrspohn, J. H. Wendorff, R. Ramesh, and M. Alexe, Appl. Phys. Lett. **83**, 440 (2003).
[11] B. A. Hernandez, K.-S. Chang, E. R. Fisher, and P. K. Dorhout, Chem. Mater. **14**, 480 (2002).
[12] E. D. Mishina, K. A. Vorotilov, V. A. Vasil'ev, A. S. Sigov, N. Ohta, and S. Nakabayashi, J. Exp. Theor. Phys. **95**, 502 (2002).
[13] Y. Luo, I. Szafraniak, V. Nagarajan, R. B. Wehrspohn, M. Steinhart, J. H. Wendorff, N. D. Zakharov, R. Ramesh, and M. Alexe, Integr. Ferroelectr. **59**, 1513 (2003).
[14] H. J. Fan, M. Knez, R. Scholz, K. Nielsch, E. Pippel, D. Hesse, M. Zacharias, and U. Goesele, Nat. Mater. **5**, 627 (2006).
[15] Y. B. Mao, S. Banerjee, and S. S. Wong, J. Am. Chem. Soc. **125**, 15718 (2003).
[16] S. J. Limmer, S. Seraji, M. J. Forbess, Y. Wu, T. P. Chou, C. Nguyen, and G. Z. Cao, Adv. Mater. (Weinheim, Ger.) **13**, 1290 (2001).
[17] J. E. Spanier, A. M. Kolpak, J. J. Urban, I. Grinberg, L. Ouyang, W. S. Yun, A. M. Rappe, and H. Park, Nano Lett. **6**, 735 (2006).
[18] G. Suyal, E. Colla, R. Gysel, M. Cantoni, and N. Setter, Nano Lett. **4**, 1339 (2004).
[19] Z. Y. Wang, A. P. Suryavanshi, and M.-F. Yu, Appl. Phys. Lett. **89**, 082903 (2006).
[20] X. Y. Zhang, X. Zhao, C. W. Lai, J. Wang, X. G. Tang, and J. Y. Dai, Appl. Phys. Lett. **85**, 4190 (2004).
[21] I. I. Naumov, L. Bellaiche, and H. X. Fu, Nature (London) **432**, 737 (2004).
[22] G. Burns and B. A. Scott, Phys. Rev. Lett. **25**, 1191 (1970).
[23] A. M. Bratkovsky and A. P. Levanyuk, Phys. Rev. Lett. **94**, 107601 (2005).
[24] A. K. Tagantsev, Phase Transitions **35**, 119 (1991).